



Comparing the cloud vertical structure derived from several methods based on radiosonde profiles and ground-based remote sensing measurements

M. Costa-Surós¹, J. Calbó¹, J. A. González¹, and C. N. Long²

¹Group of Environmental Physics, Physics Department, University of Girona, Girona, Spain

²Pacific Northwest National Laboratory, Atmospheric Measurements Laboratory, Richland, Washington, USA

Correspondence to: M. Costa-Surós (montse.costa@udg.edu)

Received: 18 February 2014 – Published in Atmos. Meas. Tech. Discuss.: 11 April 2014

Revised: 10 June 2014 – Accepted: 14 July 2014 – Published: 27 August 2014

Abstract. The cloud vertical distribution and especially the cloud base height, which is linked to cloud type, are important characteristics in order to describe the impact of clouds on climate. In this work, several methods for estimating the cloud vertical structure (CVS) based on atmospheric sounding profiles are compared, considering the number and position of cloud layers, with a ground-based system that is taken as a reference: the Active Remote Sensing of Clouds (AR-SCL). All methods establish some conditions on the relative humidity, and differ in the use of other variables, the thresholds applied, or the vertical resolution of the profile. In this study, these methods are applied to 193 radiosonde profiles acquired at the Atmospheric Radiation Measurement (ARM) Southern Great Plains site during all seasons of the year 2009 and endorsed by Geostationary Operational Environmental Satellite (GOES) images, to confirm that the cloudiness conditions are homogeneous enough across their trajectory. The perfect agreement (i.e., when the whole CVS is estimated correctly) for the methods ranges between 26 and 64 %; the methods show additional approximate agreement (i.e., when at least one cloud layer is assessed correctly) from 15 to 41 %. Further tests and improvements are applied to one of these methods. In addition, we attempt to make this method suitable for low-resolution vertical profiles, like those from the outputs of reanalysis methods or from the World Meteorological Organization's (WMO) Global Telecommunication System. The perfect agreement, even when using low-resolution profiles, can be improved by up to 67 % (plus 25 % of the approximate agreement) if the thresholds for a moist

layer to become a cloud layer are modified to minimize false negatives with the current data set, thus improving overall agreement.

1 Introduction

Clouds are a key factor driving the climate. The complexity of the processes involved, the vast amount of information needed, including spatial distribution, and the uncertainty associated with the available data, all add difficulties in determining how clouds contribute to climate change (e.g., Heintzenberg and Charlson, 2009). There is, in consequence, a general need for improvement of automatic cloud observation and continuous cloud description. Specifically, knowledge about cloud type is very important, because the overall impact of clouds on the Earth's energy budget is difficult to estimate, as it involves two opposite effects depending on cloud type (Naud et al., 2003). Low, highly reflective clouds tend to cool the surface, whereas high, semitransparent clouds tend to warm it, because they let much of the shortwave radiation through but are opaque to the longwave radiation.

The cloud vertical structure (CVS) affects the atmospheric circulation directly by modifying the radiative cooling profile and the atmospheric static stability. The effects of cloud vertical structure on atmospheric circulation have been described through the use of atmospheric models by many authors, such as Wang and Rossow (1998). Crewell et al. (2004)

underlined the importance of clouds in multiple scattering and absorption sunlight processes that, at the same time, have a significant impact on the atmospheric diabatic heating. These complex phenomena are not yet fully understood and are subject to large uncertainties. In fact, the assumed or computed vertical structure of cloud occurrence in general circulation models (GCMs) is one of the main reasons why the different models predict a wide range of future climates. For example, most GCMs underestimate the cloud cover, while only a few overestimate it (Xi et al., 2010). Therefore, to improve the understanding of cloud-related processes, and then to increase the predictive capabilities of large-scale models (including global circulation models), better and more accurate observations of both the global cloud amount and in particular of the vertical distributions of clouds are needed. The present work is a contribution towards addressing this need.

Observations and measurements are fundamental to acquiring insight regarding cloud processes. These can be performed from the ground or from a satellite. In both cases, the problem of overlapping cloud layers that hide each other is noticeable, particularly with passive observation systems. Surface observers can see most of the low clouds with or without higher clouds above them, while satellites can view most of the high clouds with or without lower clouds underneath. These limitations have hindered the development of reliable quantitative information about cloud overlap and, in general, about the vertical distributions of cloud fractions and cloud occurrence. However, ground-based and space-borne cloud radars can partially overcome this issue.

Passive satellite sensors have the advantage of providing global coverage of cloud amounts and top heights, although their retrieval accuracy suffers from various limitations. More recently, new instruments onboard satellites have been providing details about the cloud vertical structure. In particular, active sensors such as the Cloud Profiling Radar (CPR) on CloudSat and the Cloud-Aerosol Lidar with Orthogonal Polarization (CALIOP) aboard CALIPSO (Cloud-Aerosol Lidar and Infrared Pathfinder Satellite Observation) satellites are achieving notable results regarding the addition of a vertical dimension to traditional satellite images. However, because the repeat time of these polar orbiting satellites for any particular location is very large, the time resolution of such observations is low (L'Ecuyer and Jiang, 2010; Qian et al., 2012). Jin et al. (2007) recalled the importance of obtaining the cloud vertical structure by using ground-based active instruments because, in the past, satellite-based cloud data sets retrieved from passive remote sensing techniques were unable to provide the CVS. In fact, ground-based instruments such as lidar, cloud radar and ceilometers are usually applied to observe and describe the CVS. They can provide cloud measurements with high accuracy and continuous temporal coverage; however, radar and lidar are deployed at few locations around the world, and their application is limited. Ceilometers are commonly located at airports, but they

are used only for operational purposes, not for research, and have a limited range that does not cover the total troposphere. Ceilometers are very efficient at detecting clouds and can locate the bottom of cloud layers precisely, but cannot usually detect the cloud top, due to attenuation of the beam within the cloud. On the other hand, the vertically pointing cloud radar is able to detect the cloud top, although signal artifacts can cause difficulties during precipitation (Nowak et al., 2008). In this context, the Atmospheric Radiation Measurement (ARM) program developed the Active Remote Sensing of Clouds (ARSCL) product that combines data from several ground-based instruments to produce a time series of vertical distributions of cloud hydrometeors over the ARM sites (Clothiaux et al., 2000; Mather and Voyles, 2013).

The ARM locations where data from active remote sensing are combined to produce the ARSCL product are (more information in <http://www.arm.gov/>) the Southern Great Plains (SGP), near Lamont (OK); the North Slope Alaska (Central Facility in Barrow, AK); and the Tropical Western Pacific (Darwin, Australia; Manus Island, PNG; Nauru Island). The Cloudnet sites (Illingworth et al., 2007) provide a sophisticated product of vertical cloud distribution. There are nine Cloudnet observing stations across Europe equipped with a suite of active and passive remote sensing instruments (a Doppler cloud radar, a near-IR lidar ceilometer, and a dual-wavelength microwave radiometer) accompanied by standard meteorological instruments (more information in <http://www.cloud-net.org/>).

An indirect way to perform estimations of CVS is by using atmospheric thermodynamic profiles as measured by radiosondes. Radiosondes can penetrate atmospheric (and cloud) layers to provide in situ data. The vertical distributions of temperature, relative humidity and pressure measured by radiosondes are fundamental to the study of atmospheric thermodynamic and dynamic processes (Zhang et al., 2010). Actually, radiosoundings were probably the best method for obtaining the CVS from the ground before the ARSCL (and similar product) development; currently they still are the only solution to get ground-based, widespread knowledge of CVS, thanks to the network of radiosonde launching stations (around 800 worldwide). Moreover, radiosoundings are used as a reference for other upper air detection techniques (Wang et al., 2000; Eresmaa et al., 2006; Zhang et al., 2010). Nowadays, aircraft profiles are growing in number (in 2008 there were about 150 000 automated aircraft reports per day; Ballish and Kumar, 2008). The accuracy of this kind of meteorological information is of good quality and can be a valuable source of wind and temperature information for operational weather forecasting (de Haan et al., 2013). However, airplanes tend to avoid clouds, because they can be affected directly by inclement weather, so when major storms occur, airplanes often do not fly (Moninger et al., 2003). Thus, the use of aircraft in cloud-related studies may potentially introduce a bias due to biased sampling. Other matters such as the warmer temperatures usually recorded by aircraft

(Ballish and Kumar, 2008) and the trajectory of aircraft profiles (Schwartz and Benjamin, 1995) should be taken into account, if applying the methods to aircraft temperature and humidity profiles.

There are several methods available in the literature to determine the CVS from vertical thermodynamic profiles, and from radiosonde data in particular. In this study, six of these methods are applied to a number of atmospheric profiles obtained at the ARM Southern Great Plains (SGP) site, and their results are compared between them. All methods establish some conditions on the relative humidity (or closely related magnitudes, such as dewpoint depression) or its vertical variation. Some methods require a minimum vertical resolution, and some include requirements of vertical cloud layer thickness in their classification scheme. The methods examined here are those by Poore et al. (1995), Wang and Rossow (1995), Chernykh and Eskridge (1996), Dimitrieva-Arrago and Shatunova (1999), Minnis et al. (2005) and Zhang et al. (2010). These six methods are described in Sect. 2. Some authors have already performed studies of comparison between radiosonde-based cloudiness determining methods, although to our knowledge, none of these previous works has compared so many methods as done in the present study. For example, Naud et al. (2003) compared the methods by Wang and Rossow (1995) and Chernykh and Eskridge (1996), using data (November 1996–October 2000) from surface-based active sensors placed at the ARM SGP site. In the same paper, the authors checked the effect of applying different thresholds on the relative humidity for the first method and modified the second method by making it dependent on the cloud cover and altitude. They concluded that the Wang and Rossow (1995) method tends to classify moist cloudless layers as cloudy (especially at lower altitudes); furthermore, they suggested that the two methods tend to report cloud top heights that are higher than the corresponding heights from radar observations.

In a more recent comparison work, Zhang et al. (2012) conducted a campaign in China where a cryogenic frost-point hygrometer, a Vaisala RS80 radiosonde, and a GTS1 radiosonde were deployed. They compared again the methods by Wang and Rossow (1995) and Chernykh and Eskridge (1996), and adapted them to the specific behavior of every radiosonde instrument that they used. Overall, results from these earlier comparison studies have clearly demonstrated the value of radiosonde data for determining cloud vertical structure. However, they have also shown that different methods produce slightly different results, and that the cloud vertical structure derived from radiosonde data sometimes diverges from active sensor observations. These latter differences could be partly attributed to comparing retrievals from ground-based instruments, which have just a vertical view of the sky above, against CVS derived from radiosondes, which suffer a horizontal displacement due to the wind while they are ascending. In these kinds of studies, it is important to take into account possible errors associated

with different responses of different brands and models of radiosonde. Regarding this issue, Wang et al. (2003) found that Vaisala radiosonde performance is better in comparison with others like Sippican, particularly when measuring in the middle and lower troposphere. Sun et al. (2013) showed that, on average, the data from most radiosonde types produce a nighttime cold bias and a daytime warm bias relative to the Constellation Observing System for Meteorology, Ionosphere, and Climate (COSMIC) measurements. These temperature biases also vary among climate regimes and brand types. According to Sun et al. (2013), newer sondes (introduced after 2000) have smaller biases than older sondes, and appear to be less influenced by cloud effects, perhaps due to the improved sensor technology. The main objective of this study is to find the best approximation to the real CVS (as represented by ARSCL) obtained from methods based on radiosonde profiles. Methods are compared with the CVS produced by ground-based active instruments (that is, the ARSCL cloud base and top heights), so strengths and weaknesses of the methods are revealed. To illustrate the two sources of data that are combined in this study, an example of temperature and relative humidity profiles, as measured by the radiosonde and two cloud layers detected by ARSCL, is shown in Fig. 1. Geostationary Operational Environmental Satellite (GOES) images are used to address the problem of the radiosonde (RS) horizontal drift (see in Fig. 1 the sonde horizontal distance from the launching site when it reaches the altitudes where clouds are detected by ARSCL). Secondly, some improvements are suggested, and the effect of lowering the vertical resolution of profiles is analyzed (to make the method potentially useful for the outputs of reanalysis methods or for the profiles transmitted through the WMO's Global Telecommunication System).

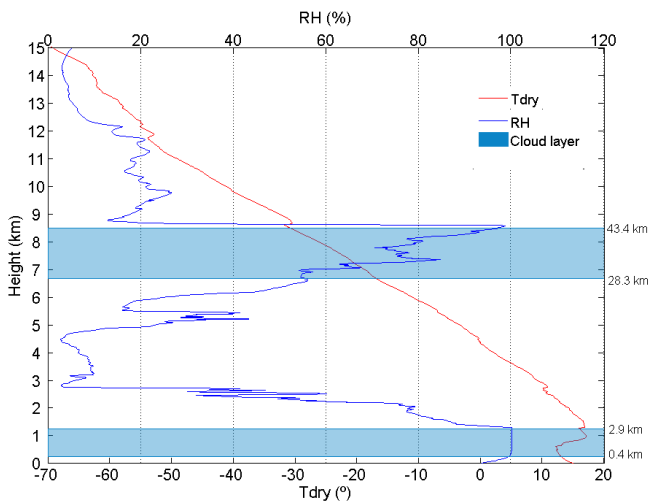
2 Data and methodology

2.1 ARSCL, radiosondes, satellite images and sky images

Data used in this study come from the Department of Energy (DOE) Atmospheric Radiation Measurement (ARM) program, specifically from the Southern Great Plains (SGP, 36°36'18.0" N, 97°29'6.0" W, 320 m a.s.l., OK, US) site. Data from 259 radiosondes (corresponding to 65 days), which are considered to be representative of all seasons of the year 2009, have been studied. Specifically, one out of approximately every five days was selected, so for each month there are 5 to 7 days. In general, four times per day are used, corresponding to the four radiosonde launches at this site. The schedule for the routine launch operations is 23:30, 05:30, 11:30, and 17:30 UTC, which corresponds to 6:30 p.m., 12:30 a.m., 6:30 a.m., and 12:30 p.m. central daylight time (CDT).

Table 1. Characteristics of instruments used as the basis of ARSCL value-added products (extracted from the corresponding handbooks from the ARM Climate Research Facility).

	VCEIL (Vaisala ceilometer CL31)	MPL (Micropulse lidar)	MMCR (Millimeter cloud radar)
Vertical range	7700 m	Up to 20 km	Up to 20 km
Maximum range for cloud base height	7500 m	18 km	
Resolution	10 m	15 m	
Wavelength	910 nm (at 25 °C)	532 nm	8.66 mm, Ka band (Frequency 34.86 GHz)
Accuracy/uncertainty	$\pm 1\%$ or ± 5 m	$\pm 2\%$	
Minimum detection height	0 m	150 m	

**Figure 1.** Temperature (T_{dry} (°), in red) and relative humidity with respect to water (RH (%), in blue) profiles above ground level from the radiosonde on 5 October 2009 at 23:23 h at SGP. Blue shading represents the cloud layers as detected by ARSCL. The values (on the right) related to every cloud layer boundary indicate the sonde horizontal distance from the ARSCL site in kilometers when it reached those altitudes.

Cloud base and top heights (CBH and CTH) are the main variables used in the present study; they are taken from the Active Remote Sensing of Clouds (ARSCL) product. ARSCL is a value-added product that combines data from active remote sensors, millimeter cloud radar (MMCR), laser ceilometer (VCEIL), and micropulse lidar (MPL), and provides a time series (with 10 s resolution) of vertical distributions of cloud hydrometeors over the ARM sites (Clothiaux et al., 2000). Both MPL and VCEIL cannot penetrate thick low-level clouds to detect any more layers of clouds aloft. However, they can detect clouds that are visible from the ground within the observation ranges, though the MPL does sometimes label layers with cloud optical thicknesses less than are typically used as a limit for human and sky imager observations. The greatest strength of the cloud radar is its ability to penetrate clouds and reveal multiple-layer

structures, but it may miss some thin clouds composed of small hydrometeors. Moreover, the detection of cloud base heights from radar is often affected by the presence of large precipitation particles, as well as insects and bits of vegetation. If such particles are suspended in the atmospheric boundary layer, this may be mistakenly regarded as stratus clouds (Clothiaux et al., 2000). The properties of the three instruments are specified in Table 1. Despite providing only a vertical “pencil” beam, cloud radar–lidar systems can provide more accurate cloud vertical distributions and compensate for most of the shortcomings in cloud vertical distributions from surface observers and even from satellite imagery (Xi et al., 2010).

One main product from ARSCL is the cloud base best estimate (CBBE), which is determined from MPL and VCEIL measurements only (no MMCR data are used). If the ceilometer first cloud base is between 0 and 3000 m, the ceilometer value is used; if the ceilometer cloud base is above 3000 m, but within 600 m of the MPL first cloud base, the ceilometer value is used. Otherwise, the MPL first cloud base is used. The difference between cloud height determination algorithms using VCEIL and MPL is that MPL uses a threshold variation to identify the cloud bottom, while the ceilometer uses a calculated vertical visibility threshold of 100 m. This means that the ceilometer will not classify thin cloud regions that MPL would identify, and will usually give a slightly higher cloud bottom height (Morris, 2012). Besides the CBBE, ARSCL provides bases and tops for up to 10 cloud layers, based on MMCR and MPL data. The best situation is when the cloud top is determined by MMCR; if this instrument is not available, the cloud top is derived from the MPL, or if the MPL beam is attenuated by the lower cloud, then it is noted as not having been retrieved. For the present study, we only use data and times where both the MPL and radar are available, giving the best possible comparison product for our purposes.

Radiosondes measure local conditions when they ascend through the atmosphere; obviously, they also produce data when they cross cloud layers. Vertical distributions of temperature, relative humidity (RH) and pressure measured by radiosondes are the fundamental values used to obtain the

cloud vertical structure by applying the six methods compared in this study. The sonde model used at the SGP Central Facility in the year 2009 was the RS92 manufactured by Vaisala. Vaisala RS92 radiosondes are the most widely used RS, and can be considered a reference nowadays (Flores et al., 2013). The used profiles have a high vertical resolution (about 10 m) as a result of the 2 s temporal resolution, and have an ascent rate in the range 2.5–5.5 m s⁻¹. Besides pressure, temperature and relative humidity, altitude, latitude, longitude, and dewpoint temperature (among others) are provided in the radiosounding files.

The radiosonde horizontal displacement, due to the drift produced by the wind, must be taken into account because it could add some difficulty when comparing the clouds detected by the RS methods with the ARSCL vertical “pencil view”. In order to address this issue, we have first represented in Fig. 2 the horizontal displacement depending on the vertical position as a boxplot diagram for the whole RS data set. At the maximum level of the low cloud base (2 km), displacements are between 0.4 and 11 km. At 6 km in height, the boundary between middle and high clouds, displacements are between 1.6 and 47 km. At 15 km in height, the horizontal distance to the launch point ranges from 1.5 to 206.3 km. The median distance steadily grows with height, reaching 79 km at 15 km. As a conclusion, the horizontal drift of the RS can be an issue when comparing with fixed instrumentation, since half of the soundings go farther than 79 km as they reach the upper levels. The horizontal positions of the RS when they reach 15 km in height are represented in the inset of Fig. 2. The RS drifts are always towards the east, due to the prevalence of the westerlies at middle latitudes.

Considering these large horizontal distances crossed by the RS, it may well happen that clouds crossed by the RS differ from clouds directly over the ARSCL site. To help screen for those RS whose trajectories go through a homogeneous cloud field, GOES images have been used to evaluate the cloudiness (or lack thereof) in the area. Geostationary Operational Environmental Satellites (GOES), operated by the United States National Environmental Satellite, Data and Information Service (NESDIS) and used by the National Weather Service (NWS), carry a five-channel (one visible, four infrared) imaging radiometer system, designed to sense radiant and solar reflected energy from sampled areas of the Earth. Here, sequences of GOES images every 15 min have been analyzed, corresponding to periods during the RS ascents. An area of 200 × 400 km² eastwards of the SGP site has been inspected. Both visible channel (band 1) images, when available, and infrared atmospheric window channel (band 4) images, have been used. Visible images make it possible to distinguish low clouds due to their high reflectance, while infrared images are more useful for detecting high clouds due to their low temperature. In addition, we check that the cloudiness derived from GOES images is compatible with what ARSCL produces over SGP. With these two conditions, some RS have been rejected from

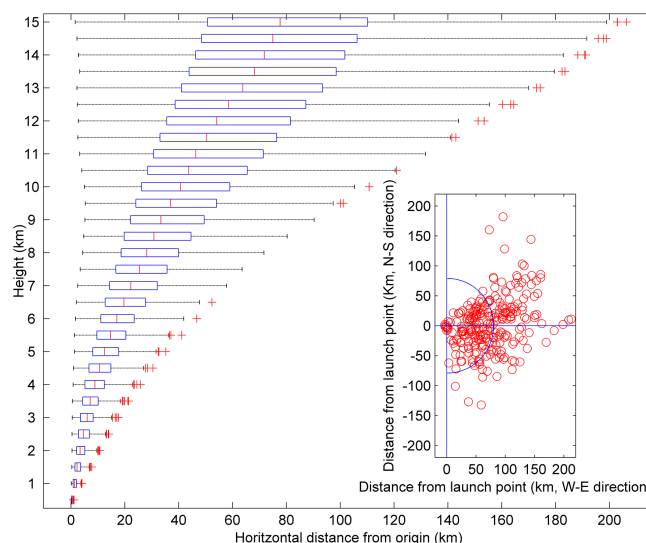


Figure 2. The boxplot shows the horizontal displacement, every 500 m in height, of the 259 radiosondes launched from SGP (the boxplot shows the minimum, the first quartile, the median, the third quartile, the maximum and, if any, observations that might be considered outliers (plus symbols)). The inset shows the horizontal projection vision of the RS position with respect to the launch point when it reaches 15 km. The semi-circle represents the median of all displacements (79 km).

the original RS database, so 193 RS out of the initial 259 RS form the suitable data set. These selected RS are still well distributed seasonally: winter 27 %, spring 21 %, summer 22 %, and autumn 30 %; they are also well distributed throughout the day: 05:30 UTC 25.4 %, 11:30 UTC 24.4 %, 17:30 UTC 26.9 % and 23:30 UTC 23.3 %. The entire procedure will be explained further by means of the examples included in Sect. 3.1.

Finally, a total sky imager (TSI-660 by Yankee Environmental Systems) provides time series of hemispheric sky images during daylight hours and retrievals of fractional sky cover for periods when the solar elevation is greater than 10°. These animated images (provided as the Supplement) add some useful information when analyzing and interpreting the results of ARSCL and radiosonde cloud vertical structure.

2.2 Cloud vertical structure estimative methods

We have considered six methods for determining CVS from radiosondes. However, as this work is based on techniques that have been developed and published earlier, we will not extensively describe their development; instead, Table 2 contains a summary of their main characteristics, and a short description is given below.

Poore et al. (1995) developed a methodology (hereinafter PWR95) with the aim of building a cloud climatology combining 14 years (1975–1988) of surface and upper-air observations (radiosoundings) at 63 sites in the Northern

Table 2. Summary of the applied RS methods.

Acronym	References	Cloud base and top height estimation methodology	Resolution (approx. number of levels)	Max. height	Data used	RH _{ice}	Min. thickness (m)	thick-	Min. CBH (m)
PWR95	Poore et al. (1995)	Temperature-dependent dewpoint depression thresholds	76 m (140)	Tropopause	z ; T_{dry} and T_{dew}	No	30.5 (low)	61 (middle, high)	No
WR95	Wang and Rossow (1995)	Two RH thresholds (minRH = 84 % and maxRH = 87 %) and 3 % jump. Sign of the second-order derivatives with respect to the height of T and RH ($T''(z)$ 0 and $R''(z)$ 0)	Low ^a (180)	10 hPa	z ; T_{dry} , P and RH	If $T < 0^\circ\text{C}$	No	No	500
CE96	Chernykh and Eskridge (1996), and Chernykh and Aldukhov (2004)	Pressure-dependent dewpoint depression thresholds	Low ^a (180)	10 hPa	z ; P , T_{dry} , T_{dew} and RH	If $T < 0^\circ\text{C}$	100	0	0
DS99	Dimitrova-Arango and Shatunova (1999)	Empirical parameterization calculating the probability of occurrence (P_{cid}) of a cloud layer using RH and T ($P_{\text{cid}}(T, \text{RH}) > 67\%$)	High ^b (3000)	300 hPa	z ; P , T_{dry} and T_{dew}	No	No	No	0
MNS05	Mirinis et al. (2005)	Improvement of the WR95 method (altitude-dependent minRH and maxRH thresholds, without the 3 % jump)	25 hPa (36)	100 hPa	z ; P , T_{dry} and RH	If $T < -20^\circ\text{C}$	No	No	0
ZHA10	Zhang et al. (2010)	Improvement of the WR95 method (altitude-dependent minRH and maxRH thresholds, without the 3 % jump)	High ^b (3000)	Top of the profile	z ; T_{dry} and RH	If $T < 0^\circ\text{C}$	30.5 (low)	61 (middle, high)	280

^a A low-resolution RS is built from the original RS (see text for details). ^b High resolution means all available data in the RS (without any transformation).

Hemisphere (0° to 80° N; 34 continental sites, 14 coastal sites, and 15 sites on islands). The main idea of the PWR95 method is to estimate the cloud base and top heights from temperature-dependent dewpoint depression thresholds. In the PWR95 method, the radiosounding processing is limited to temperatures above -40°C or at a maximum of 10 668 m above ground level (a.g.l.). The radiosounding is linearly interpolated every 76 m, and the dewpoint depression (ΔT_{d}) is calculated as the difference between the (dry) air temperature T and the dewpoint temperature T_{dew} :

$$\Delta T_{\text{d}} = T - T_{\text{dew}}. \quad (1)$$

According to PWR95, a given atmospheric level has a cloud if

$$\Delta T_{\text{d}} < 1.7^\circ\text{C} \text{ at } T > 0^\circ\text{C}$$

$$\Delta T_{\text{d}} < 3.4^\circ\text{C} \text{ at } 0 > T > -20^\circ\text{C}$$

$$\Delta T_{\text{d}} < 5.2^\circ\text{C} \text{ at } T < -20^\circ\text{C},$$

which, in terms of RH (with respect to water), is approximately equivalent to

$$\text{RH} > 91.5\% \text{ at } T > 0^\circ\text{C}$$

$$\text{RH} > 83\% \text{ at } 0 > T > -20^\circ\text{C}$$

$$\text{RH} > 74\% \text{ at } T < -20^\circ\text{C}.$$

Finally, some additional conditions are applied: a minimum cloud-layer thickness of 30.5 m (for low clouds, CBH < 1981 m) and 61 m (for middle and high clouds); cloud layers that extend to the top of the RS profile are discarded because they have indeterminate top heights.

Wang and Rossow (1995) (WR95 method) slightly modified the PWR95 method. First, for levels with temperatures lower than 0°C , RH is computed with respect to ice instead of liquid water, which allows the use of a single threshold RH at all levels. This single threshold is set to 84 % to identify a moist level; within a moist layer (i.e., several successive moist levels), the maximum RH must be greater than 87 % to be considered a cloud layer. In addition, if RH at the base (top) of the moist layer is lower than 87 %, a RH jump exceeding 3 % must exist from the underlying (above) level. All cloud layers, independent of their thickness, including single-level clouds, are retained in WR95. Another improvement is that cloud layers ending at the maximum observation altitude, which were discarded in PWR95, are kept in WR95. Finally, the minimum value of a cloud base height is set at 500 m above ground level.

The WR95 method was tested at 30 ocean sites by comparing cloud properties derived from other independent data sources (visual observations and ISCCP data). The analyzed radiosonde data correspond to the period from 1946 to 1991; the sites were selected to supplement the poor ocean coverage of the PWR95 data set. The radiosounding data set used by WR95 did not have as high a vertical resolution as the

radiosounding data from SGP that are used in the present study. For this reason, when applying the WR95 method, we have first reduced the radiosonde resolution to approximately that of the original work (that is, mandatory pressure levels, significant points, and the maximum distance between levels fixed at 200 m). The method for resolution reduction is based on Chernykh and Eskridge (1996); see immediately below.

The CE96 method (Chernykh and Eskridge, 1996), based on previous methods developed in the former Soviet Union, was evaluated using data from several United States radiosonde stations within different climates. Evaluation data were selected to include only situations where the observer could only see one cloud layer. Consequently, the evaluation is biased towards stratified cloud conditions. A few years later, Chernykh and Aldukhov (2004) further developed this method and applied it to one month of data from the Surface Heat Budget of the Arctic Ocean (SHEBA) experiment, along with satellite observations made during Phase II of the FIRE Arctic Clouds Experiment and sounding data from the National Center for Atmospheric Research (NCAR) C-130Q research aircraft.

The first step in the CE96 method is to build a new vertical profile with a lower resolution. The new, coarse profile must include these levels (with the corresponding values obtained by interpolation between the original measured values):

- Mandatory pressure levels (where $P = 1000, 925, 850, 700, 500, 400, 300, 250, 200, 150, 100, 70, 50, 30, 20,$ and 10 hPa).
- Significant levels, to avoid differences greater than 0.5°C (air temperature) and 2.5 % (relative humidity) between two consecutive levels.
- Additional levels to obtain a maximum distance of 200 m between them.

Chernykh and Aldukhov (2004) used this technique to reduce the radiosonde data resolution, and tested different values (from 100 to 700 m) for the maximum distance between levels; based on their conclusions, we have used a value of 200 m in the present work.

According to the CE96 method, the necessary condition for the existence of clouds in a given atmospheric level is that the second derivatives with respect to height (z) of temperature and relative humidity be positive and negative, respectively:

$$T''(z) \geq 0 \text{ and } RH''(z) \leq 0.$$

To calculate the second derivative, the temperature and relative humidity profiles are first approximated by cubic splines; in this way, the second derivatives can be continuously estimated over the entire vertical profile as linear functions over each segment.

Then, when the previous conditions are met in a given level, the Arabey diagram (Chernykh and Eskridge, 1996) is applied to evaluate the cloud cover in it. If cloud cover is determined to be less than 20 %, that level will not be considered cloudy. In addition, for a succession of levels accomplishing both criteria to form a cloud layer, they must total a minimum thickness of 100 m.

Chernykh and Eskridge (1996) argued that this methodology makes physical sense, because in a region of the atmosphere containing clouds, one expects higher relative humidity than in the layer above and below the cloud layer. Hence, a local maximum ($RH''(z) \leq 0$) must be reached. They also commented that clouds ordinarily have a more defined top than base and nearly always lie under a temperature inversion (so $T''(z) \geq 0$ at the cloud top). Condensation of water vapor and its accompanying release of latent heat make it reasonable for temperature to stop decreasing with height or to increase with height near the base of a cloud (hence, a local minimum, i.e., $T''(z) \geq 0$, is also expected at the cloud base).

The basis of the DS99 method (Dimitrieva-Arrago and Shatunova, 1999; L. Dimitrieva, 2012, personal communications) is the vertical distribution of dewpoint depression (ΔT_d) in the atmosphere, as in the PWR95 method. Characteristic values of dewpoint depression in clouds are known from analysis of the great number of aircraft data (mostly for stratiform clouds) conducted by specialists of the Hydrometeorological Scientific Research Center of Russia. Thus, Dimitrieva-Arrago and Koloskova (1969) carried out a comparison of cloud vertical structure (location of cloud boundaries and cloud thickness) calculated using characteristic values of ΔT_d , with real cloud distributions derived from aircraft data. From this previous study, the method is quite simple. First, the dewpoint depression must be calculated at every radiosonde level. Then, three pressure-dependent dewpoint depression thresholds are applied to find the cloud layers:

$$\Delta T_d < 1.5^{\circ}\text{C} \text{ at } 1000 \text{ hPa} > P > 800 \text{ hPa}$$

$$\Delta T_d < 2.5^{\circ}\text{C} \text{ at } 800 \text{ hPa} > P > 550 \text{ hPa}$$

$$\Delta T_d < 5^{\circ}\text{C} \text{ at } 550 \text{ hPa} > P > 300 \text{ hPa}.$$

Assuming the typical temperature found in the corresponding pressure range, ΔT_d thresholds can be expressed as RH (with respect to water) thresholds:

$$RH > 92.5 \% \text{ at } 1000 \text{ hPa} > P > 800 \text{ hPa} \text{ (at } 15^{\circ}\text{C)}$$

$$RH > 87.5 \% \text{ at } 800 \text{ hPa} > P > 550 \text{ hPa} \text{ (at } 0^{\circ}\text{C)}$$

$$RH > 75 \% \text{ at } 550 \text{ hPa} > P > 300 \text{ hPa} \text{ (at } -20^{\circ}\text{C)}$$

Minnis et al. (2005, MNS05 hereafter) provided a new cloud detection method derived from high temporal resolution ARSCL data, balloon-borne soundings, and satellite retrievals over the ARM SGP Central Facility between 1 March 2000 and 28 February 2001. MNS05 is an empirical parameterization that calculates the probability of occurrence of a cloud layer using RH and air temperature from

Table 3. Summary of the values for min-RH, inter-RH and max-RH from Zhang et al. (2010), and the new max-RH thresholds suggested for the low-resolution test.

Altitude range	ZHA10 min-RH	ZHA10 inter-RH	ZHA10 max-RH	New max-RH
0–2 km	92–90 %	84–82 %	95–93 %	93.5–91.5 %
2–6 km	90–88 %	82–78 %	93–90 %	91.5–89 %
6–12 km	88–75 %	78–70 %	90–80 %	89–77.5 %
> 12 km	75 %	70 %	80 %	77.5 %

radiosondes. First, RH values must be converted to RH with respect to ice when temperature is less than -20°C ; on the other hand, the profile has to be interpolated every 25 hPa up to the height of 100 hPa. An expression to estimate the cloud probability (P_{cld}) as a function of temperature and relative humidity is then applied; in this formula, relative humidity is given the maximum influence, since it is the most important factor in cloud formation. Finally, a cloud layer is set wherever $P_{\text{cld}} \geq 67\%$. Jin et al. (2007) slightly modified this method for its application to Arctic conditions (i.e., colder and less polluted). Minnis et al. (2005) developed their method to compare it with the Rapid Update Cycle (RUC) 40 km resolution model results (so, a different goal than the other methods presented in this section, i.e., to create cloud climatologies). We have adapted and applied it in the present study given that the method produces what we would like to analyze: the CVS from vertical thermodynamic profiles.

Zhang et al. (2010, ZHA10 hereafter) developed their methodology on the basis of data obtained during a campaign in Shouxian (China) from 14 May to 28 December 2008, where the ARM Mobile Facility (AMF) was deployed. Radiosonde data were used to analyze cloud vertical structure by taking advantage of the first direct measurements of cloud vertical layers from the 95 GHz radar. The ZHA10 method is clearly an improvement on the WR95 method. Instead of a single WR95 threshold, ZHA10 is based on altitude-dependent thresholds without the requirement of the 3 % RH jump at the cloud base and top. Threshold values depending on height are shown in Table 3. According to their own results, Zhang et al. (2010) concluded that cloud layers retrieved using the ZHA10 method agree well with the surface active remote sensing observations (cloud radar, MPL, ceilometer) of cloud vertical distributions (the absolute differences in cloud base heights from radiosonde and MPL/ceilometer comparisons are less than 500 m for 77.1 %/68.4 % of the cases analyzed).

As a first step, the RH with respect to liquid water is converted to RH with respect to ice when the temperature is below 0°C . Then, moist layers are identified by applying four conditions: (a) the base of the lowest moist layer is determined as the level where RH exceeds the minimum RH threshold (min-RH) corresponding to this level, (b) above the base of the moist layer, contiguous levels with RH over the

corresponding min-RH are treated as the same layer, (c) the top of the moist layer is identified where RH decreases below the corresponding min-RH, and (d) moist layers with bases lower than 120 m and thicknesses less than 400 m are discarded. Subsequently, cloud layers are defined through four additional steps: (a) a moist layer is classified as a cloud layer if the maximum RH within this layer is greater than the corresponding maximum RH (max-RH) at the base of this moist layer, (b) the base of cloud layers is set to 280 m a.g.l., and cloud layers are discarded if their tops are lower than 280 m, (c) two contiguous layers are considered a single layer cloud if the distance between these two layers is less than 300 m or if the minimum RH within this distance is greater than the maximum inter-RH value, and (d) clouds are discarded if their thicknesses are less than 30.5 m for low clouds and 61 m for middle/high clouds.

As stated in the introduction, the particular formulation and thresholds of each method may be influenced by the specific brands/models of sonde used. PWR95 and WR95 use rawinsonde observations (RAOBS) data, without specifying RS brands or models; CE96 use the Comprehensive Aerological Reference Data Set (CARDS) data set and mention the VIZ radiosonde; DS99 use aircraft measurements; and MNS05 and ZHA10 use different models of Vaisala RS (RS80-15LH and RS92, respectively).

2.3 Methodology

First, the radiosonde trajectory (only the vertical position is considered) is graphically superposed to the temporal evolution of ARSCL CBBE and the first three CBH and CTH. From this representation, heights of cloud bases and tops are extracted by a visual inspection, obtaining what we call ARSCLv heights, which correspond to cloud bases and tops eventually crossed by the sonde during its ascent. These values will be the main reference considered in the present study for comparison. Additionally, the mean value of ARSCL cloud bases and tops is calculated, from the time when the RS is launched until half an hour later, and will be denoted as ARSCLm. It has to be noted that the CBBE (from VCEIL/MPL) is considered the first cloud base layer, unless the first CBH (from MMCR/MPL) is lower.

Then, the next step is to compare the behavior of the six methods described above with ARSCL observations. First, the sky situations were classified into four categories (according to ARSCLv): “No clouds”, “1 layer”, “2 layers”, or “More than 2 layers”. Then, for every sky situation, the methods were classified into several categories, depending on the correspondence between the methods and the observations. Furthermore, every case was labeled as “False negative”, “False positive”, “Perfect agreement”, “Approximate agreement”, or “Not coincident”, defined as follows.

“False negative” means that no clouds were detected by the method when ARSCLv gives one or more cloud layers. “False positive” means that one or more cloud layers were

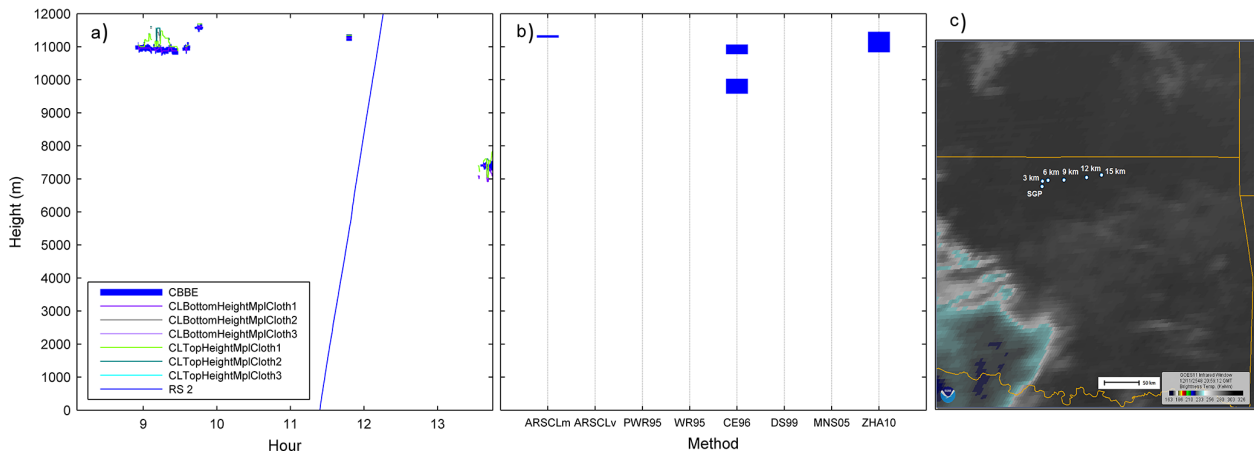


Figure 3. Case 1: 15 April 2009, no clouds. **(a)** Vertical position of the radiosounding depending on the time and the ARSCL products around the RS launch time (11:21 UTC). **(b)** Cloud layers as detected by ARSCL (ARSCLm and ARSCLv), and as found by the explained methods (PWR95, WR95, CE96, DS99, MNS05 and ZHA10). **(c)** GOES image in the infrared channel at 12:00 UTC (approximately 30–45 min from the launch time). Dots indicate the horizontal position of the RS every 3 km in height.

detected by the method when ARSCLv does not give any cloud. “Perfect agreement” occurs when the method detects the same cloud layer/s (number and heights) as ARSCLv. “Approximate agreement” occurs when the method correctly detects at least one layer that ARSCLv gives, but disagrees on the whole cloud vertical structure. Finally, all other cases are labeled as “Not coincident”.

Regarding the matching between heights of cloud layers, the first step is to classify cloud layers (both from ARSCLv and the RS methods) as “Low” ($CBH < 2000$), “Middle” ($2000 \text{ m} < CBH < 6000 \text{ m}$) or “High” ($CBH > 6000 \text{ m}$) (according to the World Meteorological Organization, 1975). To classify the layers derived from the RS methods, a tolerance interval from $\pm 300 \text{ m}$ to $\pm 500 \text{ m}$ is admitted when CBH is near a boundary (2000 m or 6000 m, respectively). Secondly, an RS layer is considered coincident to the ARSCLv layer if it belongs to the same class (low, middle or high), and (i) if the ARSCLv cloud layer and the RS cloud layer are partly or totally superimposed on each other, or (ii) if the CBH from the RS method does not differ for more than 150 m (low clouds), 300 m (middle clouds) or 600 m (high clouds) from the ARSCLv CBH.

3 Results and discussion

3.1 Case studies

Before presenting general results for the whole data set, we present here in detail four of the analyzed cases, corresponding to different sky situations (no clouds, low clouds, middle clouds, and clouds in two layers, respectively). Figures 3 to 6 are composed of (a) the ARSCL and RS plots, (b) the cloud layers resulting from every applied method, and (c) GOES infrared images corresponding to approximately 30–45 min

after the launch time (the SGP location and the position of the RS every 3 km in height are indicated in these images). Additionally, TSI animations for each case study (only available for daytime situations) are available in the Supplement. All these figures and procedures allow guessing if the sonde may have crossed a cloud layer. In particular, taking into account the horizontal projection of the ascending RS, GOES images help to guess whether the trajectory of the RS had clouds.

Specifically, panels (a) of Figs. 3–6 show the ARSCL products around the RS launch time, that is the Cloud Base Best Estimate (CBBE), and up to three bottom heights and top heights of hydrometeor layers from composite MMCR/MPL. The vertical position of the radiosounding depending on the time is shown in the same panel, so it is easy to visualize if cloud layers were constant or not directly above the SGP during and around the RS ascent. Panels (b) show, first of all, the cloud layers as detected by ARSCL (ARSCLm and ARSCLv), and second, the cloud layers found with the explained methods (PWR95, WR95, CE96, DS99, MNS05 and ZHA10).

Figure 3a, corresponding to 15 April 2009, shows that during the RS ascent, there were no clouds above the site (except for a tiny high cloud at around 11:40 UTC). This is supported by TSI animation images (Supplement). Moreover, GOES images confirm that the RS moved through a region free of clouds (see Fig. 3c). Despite this, Fig. 3b shows that some methods (CE96 and ZHA10) detect high clouds (producing a false positive); therefore, these two methods find a moist layer, which could possibly be related to clouds present earlier, or moisture at that level downstream of the ARSCL location that the RS passed through, and which interpreted it as a cloud. The other methods do not detect any cloud layers, as it

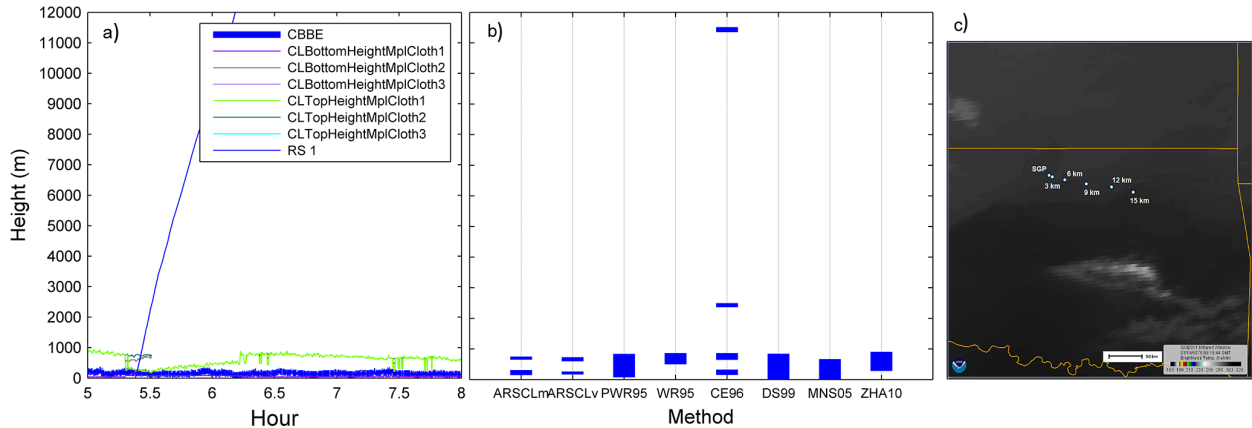


Figure 4. Idem as Fig. 3, but for Case 2: 15 October 2009, low clouds. RS launch time: 05:23 UTC. GOES infrared image at 06:00 UTC.

should be, according to ARSCL and satellite images (perfect agreement).

In Fig. 4a (15 October 2009), ARSCL data show that during the RS ascent, there are two low, thin cloud layers below 1000 m, although the higher layer disappeared at 05:30 UTC. Probably, the RS crossed these two layers, since the horizontal displacement during the few minutes that are needed by the RS to reach 1000 m is very small (see Fig. 4c). Despite a relatively large maximum horizontal displacement, GOES images confirm that the RS moved through a region of homogeneous low clouds (Fig. 4c), so this profile is maintained in the data set. Note that these low clouds, which have a temperature similar to surface, are hardly distinguishable in a static infrared image, but become perceptible when the image sequence is inspected. Only the CE96 method (Fig. 4b) detects these two layers, but it also finds other layers at the middle and high levels of the troposphere that did not exist (therefore it is an approximate agreement). All other methods are also in approximate agreement with ARSCL, because they detect the two layers as one layer.

For the case in Fig. 5a (10 July 2009), ARSCL observed a cloud layer at about 5 km over SGP during the RS ascent, but PWR95 is the only method that detected it (Fig. 5b), showing a perfect agreement. The other methods give false negatives. The TSI animation of that day (Supplement) shows that, at the launch time (11:30 UTC) and also at the time when the RS reached 5 km (11:48 UTC), there are scattered clouds at SGP. GOES images show that the RS moved through a region with inhomogeneous mid-level cloudiness (Fig. 5c), so for this reason, this profile is not included in the database. In fact, this case could be an example of what Naud et al. (2003) already found: the disagreements between radar- (in our study, ARSCL) and radiosonde-derived cloud boundaries may be caused by broken cloud situations when it is difficult to verify that fixed active sensors and radiosondes are observing the same clouds due to the horizontal drift of the latter.

For the case in Fig. 6 (5 October 2009), ARSCL detected two cloud layers: a low cloud layer (from 250 to 1200 m) and a high layer (from 6700 to 8500 m) during the ascent of the RS. The PWR95, WR95, DS99 and ZHA10 methods detected the two cloud layers that ARSCL observed as well, so they are classified as “Perfect agreement”. CE96, DS99 and MNS05 are classified as “Approximate agreement”, because CE96 detected two low layers, DS99 detected an additional high layer, and MNS05 only detected the low layer. The TSI animation (Supplement) from 23:28 UTC (RS launch time) to 00:00 UTC shows that there are clouds over the location, and also some raindrops. This case is included in the database, since the GOES image 47 min after the RS launch (Fig. 6c, from 6 October 2009 at 00:15 UTC) confirms that some clouds were present over SGP and over the region where the RS moved through.

3.2 General results

Table 4 summarizes the behavior of the six methods for cloud detection from radiosoundings when compared to ARSCL observations, for all the 193 profiles considered. The sky situations are classified into four categories using ARSCL data: “No clouds” (94 cases), “1 layer” (58), “2 layers” (32), or “More than 2 layers” (9). Then, for every sky situation, the methods are classified into several categories, depending on the coincidence with the number and position of observed layers. Furthermore, every comparison is accounted as “False negative”, “False positive”, “Perfect agreement”, “Approximate agreement”, or “Not coincident”, as previously defined. The 95 % confidence intervals are also given for perfect agreement as an estimation of the statistical uncertainty ($\pm 7\%$).

According to the results in Table 4, three methods (PWR95, MNS05 and ZHA10) have perfect agreements greater than 50 %. Two of these methods (PWR95 and ZHA10) stand out for their high perfect agreements of 50.3 % and 53.9 %, and high approximate agreements of 35.8 % and

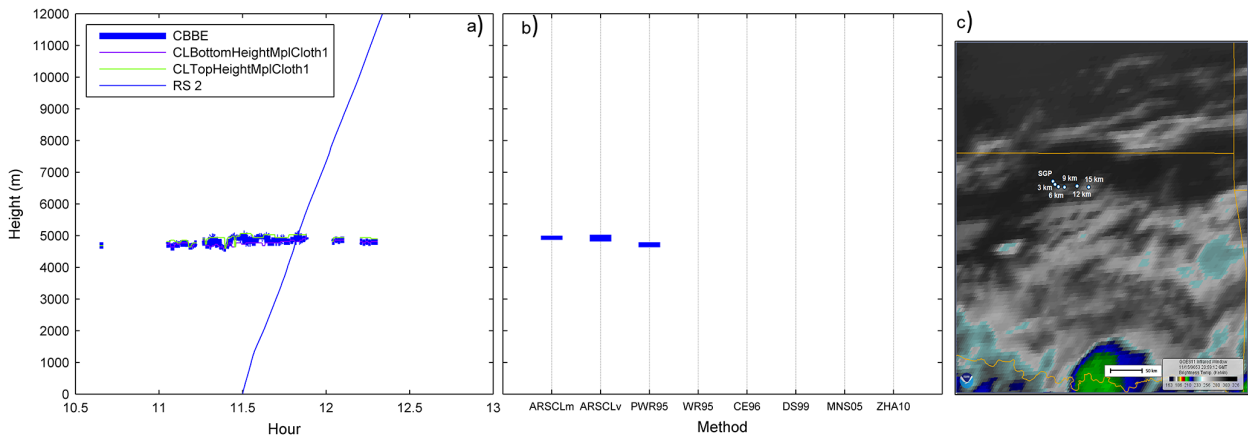


Figure 5. Idem as Fig. 3, but for Case 3: 10 July 2009, middle clouds. RS launch time: 11:30 UTC). GOES infrared image at 12:00 UTC.

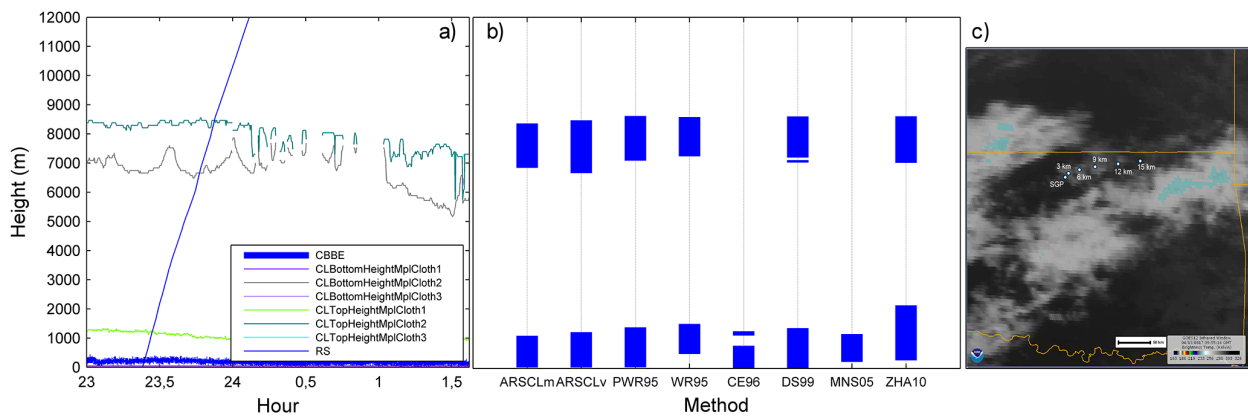


Figure 6. Idem as Fig. 3, but for Case 4: 5 October 2009, two layers of clouds: low and high clouds. RS launch time: 23:28 UTC. GOES infrared image at 00:15 UTC (6 October 2009).

29.5 %, respectively, meaning that less than 17 % of the cases may be considered incorrect (“False positive”, “False negative”, “Not coincident”) for both methods. MNS05 presents a very high ratio of perfect agreement (64.2 %), but it gives false negative detections very often (that is, the method does not detect clouds in 18.1 % of cases), so its approximate agreement is also very low (15.0 %). The poorest results are obtained by CE96 (perfect agreement 25.9 %), which detects many layers that do not exist (for example, 24.4 % false positive, and 20.7 % not coincident with any ARSCL layer). Finally, if the analysis is done only with the cloudy situations (so, without considering the “No clouds” cases), the perfect agreement worsens in all methods, as expected, considering that the cloudless cases are the simplest. ZHA10 only reduces its perfect agreement to 32 %, while at the other extreme, CE96 decreases its perfect agreement to 1 %. However, the proportion of approximate agreement increases remarkably for all methods. In particular, PWR95, WR95 and DS99 improve their approximate agreement up to values from 70 to 80 % (not shown in Table 4).

It is remarkable that the DS99 method is quite efficient despite its simplicity and the fact that it was developed mainly from stratiform situations. This method produces the highest number of approximate agreements (40.9 %), due to a number of cases in which more layers than are actually in existence (according to ARSCL) are detected. For example, from the 58 one-layer cases, DS99 detects this layer correctly in 56 cases, and at least one more layer in 45 of these. Similarly, from the 32 two-layer cases, DS99 detects both layers in 19 cases, but at least one more layer in 14 of them.

The major problem with MNS05 is that it tends to underestimate the presence of clouds in many situations (e.g., 20 out of 58 one-layer cases, 25 out of 32 two-layer cases); for this reason, its false negative percentage is high (18.1 %) in comparison to the other methods. Accordingly, there are very few false positives from MNS05 (0.5 %), while all other methods have significantly higher values (from 10.9 to 24.4 %). For these reasons, MNS05 worsens noticeably when only cloudy situations are considered.

Table 4. Behavior of the six RS methods for cloud detection compared to ARSCL observations. Data in bold account for “Perfect agreement” cases; data in italics account for “Approximate agreement” cases.

ARSCL (Visu)			Situation	METHOD						
Situation	No. of cases	%		PWR95	WR95	CE96	DS99	MNS05	ZHA10	
No clouds	94	48.7	No clouds	73	67	49	69	93	72	
			Clouds (1st CBH)	Low	12	10	18	10	1	6
				Middle	9	12	7	13	0	6
				High	0	5	22	2	0	10
1 layer	58	30.1	No clouds	1	1	5	1	20	4	
			1 layer	21	16	1	11	27	29	
			Not coincident	2	0	8	1	1	2	
			> 1 layer	33	40	17	45	9	23	
			Any coincidence	1	1	25	0	1	0	
2 layers	32	16.6	No clouds	1	1	2	0	11	1	
			1 layer	5	8	1	4	12	10	
			No coincidence	0	0	1	0	2	0	
			2 layers	3	5	0	5	4	3	
			One is coincident	6	1	2	1	2	5	
			Any coincidence	0	0	1	1	0	1	
			> 2 layers	7	4	14	7	1	7	
One is coincident	10	13	7	14	0	5				
Any coincidence	0	0	4	0	0	0				
> 2 layers	9	4.7	No clouds	1	0	2	0	4	2	
			Perfect agreement	0	0	0	0	0	0	
			<i>Approximate agreement</i>	8	9	6	8	5	7	
			Any coincidence	0	0	1	1	0	0	
			False negative	1.6 %	1.0 %	4.7 %	0.5 %	18.1 %	3.6 %	
			False positive	10.9 %	14.0 %	24.4 %	13.0 %	0.5 %	11.4 %	
			Not coincident	1.6 %	0.5 %	20.7 %	1.6 %	2.1 %	1.6 %	
			<i>Approximate agreement</i>	35.8 %	38.9 %	24.4 %	40.9 %	15.0 %	29.5 %	
			Perfect agreement ± CI*	50.3 ± 7.1 %	45.6 ± 7.0 %	25.9 ± 6.2 %	44.0 ± 7.0 %	64.2 ± 6.8 %	53.9 ± 7.0 %	

* CI: confidence interval of perfect agreement at 95 % confidence.

The CE96 method stands out for its false positive detections: the method produces more cloud layers than observed in 47 out of 94 no-cloud cases, 42 out of 58 one-layer cases, and 25 out of 32 two-layer cases; it seems that this method is too sensitive. Zhang et al. (2012) found the same behavior for CE96, and remarked that this method identifies too many very thin cloud layers (our results indicate that CE96 detects high clouds in 23 % of the no-cloud cases). In fact, Seidel and Durre (2003) had already criticized the use that Chernykh et al. (2001) made of the CE96 method to analyze the trends in low and high cloud boundaries using radiosonde data obtained from 795 stations around the world. Specifically, Seidel and Durre (2003) claimed that (1) the CE96 method is very sensitive to vertical resolution, and (2) that the vertical resolution of soundings has increased over recent decades, and concluded that these limitations “undermined the credibility of the reported trends”. Subsequently, Chernykh et al. (2003) replied to these criticisms, arguing that the calculations in Chernykh et al. (2001) were accurate enough, so that the obtained trends represent atmospheric changes that are possibly due to climate change.

When the database is analyzed seasonally, some interesting facts appear; the perfect agreement for each method and season is presented in Table 5. As can be seen in this table, the inter-seasonal variation in perfect agreement is greater than 30 % for MNS05 and DS99, indicating that these methods have a distinct seasonal behavior. All methods show the maximum perfect agreement in winter, except for the CE96 method. This is due to the high number of “No clouds” situations in winter (71 %), which in general are correctly identified. The good performance of the WR95, PWR95, DS99 and ZHA10 methods when the clear sky cases are not considered is quite stable across the year (not shown).

3.3 ZHA10 tests and improvements

ZHA10 is an improvement of WR95, which in its turn is a modification of PWR95. The original reference to the ZHA10 method (Zhang et al., 2010) presents a detailed comparison with cloud radar measurements that give the reference CVS, while the two earlier methods were compared against surface visual observations (and ISCCP data), which can hardly give an accurate description of the cloudiness

Table 5. Seasonal values of perfect agreement (in parentheses, the total number of cases) and its maximum difference for each method (W: winter. Sp: spring. Su: summer. A: autumn).

Method	Perfect agreement (%)				Max. variation (%)
	W (52)	Sp (41)	Su (42)	A (58)	
PWR95	59.6	41.5	59.5	41.4	18.2
WR95	53.8	41.5	52.4	36.2	17.6
CE96	28.8	19.5	35.7	20.7	16.2
DS99	65.4	31.7	42.9	34.5	33.7
MNS05	84.6	48.8	64.3	56.9	35.8
ZHA10	69.2	41.5	54.8	48.3	27.7

structure. Our analyses produce similar results regarding these three methods, where the perfect agreement for ZHA10 is better than for PWR95 and WR95 (Table 4), and also when only cloudy situations are considered. In addition, a slight change in the ZHA10 method produces a noticeable improvement in its performance (see below). Therefore, we have tested this method's suitability for low-resolution vertical profiles, and have checked the algorithm conditions for a moist layer to become a cloud layer and the conversion of relative humidity with respect to ice, besides the effect of coarsening RS vertical resolution.

The original ZHA10 method gives a relatively high number of false positive detections, in particular for thin clouds. Therefore, in order to reduce this percentage, we extended to the whole atmospheric profile the condition of the minimum thickness (400 m) of a moist layer to be considered a cloud layer. Recall that ZHA10 applies this condition only to moist layers with bases lower than 120 m. As expected, this new method, which will be denoted as ZHA10i, reduces false positive detections from 11.4 % to 8.8 %, and improves the perfect agreement from 53.9 % to 60.1 %, (see Table 6). This improvement is mainly linked to a better detection ("Coincident") of one-layer cases (35 out of 58), and is spread along all seasons and when only cloudy situations are considered.

Several studies (including methods ZHA10, WR95, and MNS05, but also Yi et al., 2004, for example) remark on the calculation of the relative humidity with respect to water or to ice when the temperature is low enough. Therefore, we perform two tests: (1) removing the conversion of RH with respect to ice (ZHA10i-a); or (2) lowering the threshold temperature from 0 to -20°C (ZHA10i-b). As can be seen in Table 6, the overall behavior of these two tests is worse than ZHA10i. In fact, ZHA10i-a is less effective in general than ZHA10i: it loses more layers (especially high cloud layers), which increases the false negative detections (from 3.6 % to 12.4 %), resulting in a perfect agreement improvement of 60.1 % to 63.7 %, but an approximate agreement reduction from 26.4 % to 19.2 %. With ZHA10i-b, for the whole year, neither the perfect agreement nor the approximate agreement changes much with respect to ZHA10i. However, results of

ZHA10i-b are seasonally dependent: agreements for winter and spring are better than for ZHA10i, and for autumn and summer they are worse. Therefore, further analyses and tests will be performed on ZHA10i, without any change regarding the treatment of relative humidity with respect to ice.

Despite the high vertical resolution of the current RS measurements, most sonde launching sites around the world release low vertical resolution profiles (GTS messages), so it is good to know if the ZHA10i method works for lower resolutions as well. It could be useful to check if this method could be used in reanalysis products. Reanalysis gives results at a coarse vertical resolution (see, for example, Table 2 in Crewell et al., 2004, or Table 1 in Illingworth et al., 2007). Specifically, the typical number of levels in the models and reanalyses is in the range of 30–60 (that is, a resolution of around several hundred meters or several tenths of hectopascals), while the typical number of levels in radiosoundings is on the order of several thousands (that is, as previously mentioned, a resolution of a few meters, or about one hectopascal). Therefore, we downgraded the resolution of the radiosoundings by using the procedure from Minnis et al. (2005) to decrease the vertical resolution to 25 hPa (that is, from around 3000 to 36 levels), and then applied the ZHA10i method.

Results of this test (ZHA10iLR hereinafter) show that the perfect agreement is significantly higher than ZHA10i (increasing from 60.1 to 66.3 %). Combining perfect and approximate agreements, ZHA10iLR shows low variability along the year, with the minimum in summer (perfect 66.7 %, approximate 16.7 %) and the maximum in winter (perfect 86.5 %, approximate 5.8 %). We also find that false negative situations increase (from 3.6 to 7.8 %), while false positive detections decrease (from 8.8 to 1 %). Therefore, the use of a lower resolution (ZHA10iLR) does not imply poorer results; contrarily, in many situations the detection of cloud layers improves.

ZHA10iLR results were inspected in detail, and we found that the method tends to produce fewer cloud layers (which can explain the transfer from false positive detections towards false negative detections), while the layers found tend

Table 6. Behavior of the tests performed on the ZHA10 method compared to ARSCL observations. Data in bold account for “Perfect agreement” cases; data in italics account for “Approximate agreement” cases.

ARSCL (Visu)			Situation		METHOD					
Situation	No. of cases	%			ZHA10	ZHA10i	ZHA10i-a	ZHA10i-b	ZHA10iLR	ZHA10 LRnew
No clouds	94	48.7	No clouds		72	77	90	79	92	90
			Clouds (1st CBH)	Low	6	4	2	4	1	2
				Middle	6	6	2	3	0	0
				High	10	7	0	8	1	2
1 layer	58	30.1	No clouds		4	5	16	6	12	7
			1 layer	Coincident	29	35	31	33	34	36
				Not coincident	2	0	1	1	3	0
			> 1 layer	<i>Some is coincident</i>	23	18	10	17	9	15
				Any coincidence	0	0	0	1	0	0
			2 layers	32	16.6	No clouds		1	1	5
1 layer	<i>One is coincident</i>	10				12	14	13	18	17
	No coincidence	0				0	4	0	0	0
2 layers	Coincident	3				4	2	3	2	3
	<i>One is coincident</i>	5				5	1	5	5	4
	Any coincidence	1				2	0	2	0	1
> 2 layers	9	4.7	<i>One is coincident</i>	7	3	3	3	3	3	
			<i>Two are coincident</i>	5	5	3	5	2	2	
			Any coincidence	0	0	0	0	0	0	
			No clouds	2	1	3	1	1	1	
> 2 layers	9	4.7	Perfect agreement		0	0	0	0	0	0
			<i>Approximate agreement</i>	7	8	6	8	8	8	
			Any coincidence	0	0	0	0	0	0	
			False negative	3.6%	3.6%	12.4%	4.1%	7.8%	5.2%	
			False positive	11.4%	8.8%	2.1%	7.8%	1.0%	2.1%	
			Not coincident	1.6%	1.0%	2.6%	2.1%	1.6%	0.5%	
<i>Approximate agreement</i>	29.5%	26.4%	19.2%	26.4%	23.3%	25.4%				
Perfect agreement ±CI*	53.9 ± 7.0 %	60.1 ± 6.9 %	63.7 ± 6.8 %	59.6 ± 6.9 %	66.3 ± 6.7 %	66.8 ± 6.6 %				

* CI: confidence interval of perfect agreement at 95% confidence.

to be thinner (which make them more similar to the ARSCL reference). There are three reasons for this behavior: first, some moist layers were not found, because the interpolated (averaged) RH values of the low-resolution profile do not reach the min-RH threshold; second, some moist layers were not defined as cloud layers, because the max-RH threshold that the method fixes within the layer is not reached. This is caused, in both cases, by the averaging of the RH values involved when coarsening the resolution, which implies a smoothing of the RH vertical profile. The third reason is that some moist layers were not considered cloud layers, because the thickness threshold (> 400 m) is harder to accomplish in the low-resolution profile.

To overcome these issues, we tried to improve the ZHA10iLR method. First, we removed the condition on minimum cloud thickness (> 400 m) that we applied in ZHA10i. This means that no restriction on cloud layer thickness is imposed; note, however, that the low-resolution profile implies that even a single-layer cloud has a thickness of at least 25 hPa (i.e., 200 m at lower levels of the atmosphere, or 1000 m at the higher levels). Second, the max-RH thresholds applied in the original ZHA10 method were slightly reduced, to make the condition for a moist layer to become a

cloud layer less restrictive. The new values are given in Table 3. In fact, the effect of RH thresholds in the retrieval of CVS (in relation to different climates or different radiosonde instruments) has been discussed in previous studies (Wang et al., 1999; Naud et al., 2003; Zhang et al., 2012, among others). Moreover, Zhang et al. (2013) present a study about the suitable thresholds to be used, depending on the particular RS used and on the specific site. The test with these two changes is labeled as ZHA10LRnew in Table 6. The perfect agreement rises up to 66.8%, and the false negative detections decrease down to 5.2%, so it appears that, with these modifications, the method suggested by Zhang et al. (2010) has the potential to be applied successfully to low-resolution profiles. Note that these results are in fact slightly better than those obtained by ZHA10i in the high-resolution profile, so we also tested the change of the max-RH threshold in this case, but the results (not shown) turned out to be somewhat worse. In summary, the original values of max-RH seem adequate for high-resolution profiles, while the new thresholds suggested here appear more suitable for low-resolution profiles.

4 Conclusions

Six methods to detect cloud layers from thermodynamic vertical atmospheric profiles have been applied to 193 radiosoundings from the SGP ARM site to find the cloud vertical structure; their performance has been assessed by comparison with ARSCL data taken as a reference. Since large horizontal displacements can be achieved by the RS during their ascent, and in order to assure the homogeneity of the cloud field in the region, so that a suitable comparison can be made, GOES images have been used to screen the RS database.

Three of the methods (PWR95, WR95, and ZHA10) perform reasonably well, giving perfect agreements in around 50 % of the cases and approximate agreements in around 30 % of the cases. The other methods give poorer results (lower perfect and/or approximate agreement, and higher false positive, false negative or not coincident detections). When only cloud situations are considered, the latter methods produce even poorer results.

Ideal conditions for comparing measurements with estimations (e.g., RS totally vertical, RH and T measurements without any error, completely stationary meteorological situations) do not exist. It is obvious that none of these conditions can ever be accomplished: during the ascent, RS always suffers some horizontal displacement; all measurements bring some uncertainty; and the atmosphere is continuously changing. Therefore, despite the effort towards selection of homogeneous cloudiness cases, some disagreements could be attributed to the physical horizontal displacement of the sondes from the atmosphere directly above the ARSCL site. Using the satellite data has eliminated cases when there just were no clouds at the ARSCL detected height where the sonde ended up at that height, but there might still be some error the other way, and there may be cloud where the sonde is, but with no guarantee that it is at the same height as the ARSCL cloud.

Then, despite the good agreements found for PWR95, WR95, and ZHA10, there are still some 15 % of cases where these methods fail to estimate the CVS. In particular, there are a number of “False negative” and “False positive” cases. Disagreements correspond to cases where (1) the instruments (ARSCL) classify cloud layers that some radiosounding methods fail to detect, and where (2) some of these radiosounding methods are capable of detecting moist layers in the atmosphere that the instruments (ARSCL) do not classify as a cloud layer, but that may be potential cloud air masses because of their high relative humidity (so they might be forming or dissipating clouds). This is not surprising in the case of subvisual clouds and given the lack of a refined physical definition, i.e., threshold, of what constitutes a cloud.

The ZHA10 method is the most recent version of the treatment initially proposed in PWR95 and WR95, and provides good enough results (a perfect agreement of 53.9 % and an approximate agreement of 29.5 %) to be selected for further tests and improvements. Thus, several tests were performed

on this method by changing (1) the minimum thickness for a moist layer to be considered a cloud layer, (2) the threshold temperature to calculate RH with respect to water or with respect to ice, (3) the resolution of the atmospheric profile, and (4) the altitude-dependent thresholds used to distinguish between moist and cloud layers. We found that extending the condition of a minimum thickness for a cloud results in an overall improvement of the method (perfect agreement 60.1 %; approximate agreement 26.4 %), but that modifying the RH calculations does not produce any improvement.

A notable result of the present study comes from the tests performed with low-resolution profiles. Slightly modifying the RH thresholds and again removing the condition of minimum cloud thickness (ZHA10LRnew method) allows the achievement of better overall results (perfect agreement 66.8 %; approximate agreement 25.4 %) than those obtained by the original method, even when it was applied to high-resolution profiles. It appears that the method suggested by Zhang et al. (2010) (and conveniently modified) may be applied successfully to lower-resolution profiles such as the GTS vertical profiles, or to the reanalysis temperature and humidity products, to see if clouds are produced as well, to compare with the reanalysis data. For example, an estimate of the CVS from RS or from computed atmospheric profiles may be needed for applications such as radiative transfer, agrometeorological or weather forecast studies.

The present study extends previous comparison studies on RS methods used to obtain CVS, such as those by Naud et al. (2003) and Zhang et al. (2012), since it considers more methods and accurately compares retrievals (layer by layer) against a reliable reference (ARSCL) and for an accurately selected set of cases. For example, Naud et al. (2003) found that WR95 and CE96 were generally consistent, but their analysis was limited to the lowest cloud bases and highest cloud tops. Obviously, it would be of interest to extend our analyses to other sites (other climate regimes, such as tropics and arctic regions), other data sets (e.g., aircraft profiles from the Aircraft Communications, Addressing, and Reporting System, ACARS), or other references (such as those provided by satellite platforms, i.e., CloudSat and CALIPSO, or by other projects like Cloudnet). When using other references with the aim of testing or comparing the retrieved CVS, the horizontal mismatch between the profile and the reference instruments (both ground or satellite based) should be taken into account. Other further improvements of the methods for deriving cloud vertical structure from radiosoundings (for example, by including other variables such as vertical velocity) should also be addressed as a priority.

If these methods are to be applied widely to build climatologies of CVS, the issue of different brands and models of sondes must be addressed; similar caution should be taken into account when using aircraft profiles. In addition, the present study has shown that any of the methods is good enough to be used in climatologically oriented studies if a high accuracy of the CVS is sought. However, the results

of the present paper are useful because they quantitatively assess the ability of the methods based on radiosoundings, which have been applied in the past in several studies; in addition, this research clearly shows which are the best methods, and even suggests an improvement to one of them.

The Supplement related to this article is available online at doi:10.5194/amt-7-2757-2014-supplement.

Acknowledgements. This research was funded by the Ministerio de Ciencia e Innovación of the Spanish Government through grants CGL2007-62664 (NUCLIEREX) and CGL2010-18546 (NUCLIERSOL). M. Costa-Surós was supported by research fellowship FPI BES-2008-003129 from the Ministerio de Ciencia e Innovación of the Spanish Government. C. N. Long acknowledges support from the Office of Science of the US Department of Energy as part of the Atmospheric Systems Research (ASR) program. Data and TSI animations were obtained from the Atmospheric Radiation Measurement (ARM) program sponsored by the US Department of Energy. We thank L. Dimitrieva-Arrago for her explanations and interesting discussions while visiting the University of Girona in the framework of the UE CLIMSEAS project (FP7-PEOPLE-2009-IRSES proposal no. 247512). We also thank the National Oceanic and Atmospheric Administration (NOAA) Comprehensive Large Array-data stewardship system (CLASS) for providing GOES images for research use.

Edited by: A. Macke

References

- Ballish, B. and Kumar, V. K.: Systematic differences in aircraft and radiosonde temperatures, Implications for NWP and Climate Studies, *Bull. Am. Meteorol. Soc.*, 89, 1689–1708, doi:10.1175/2008BAMS2332.1, 2008.
- Chernykh, I. and Aldukhov, O.: Vertical distribution of cloud layers from atmospheric radiosounding data, *Izv. Atmos. Ocean. Phys.*, 40, 41–53, 2004.
- Chernykh, I. and Eskridge, R.: Determination of cloud amount and level from radiosonde soundings, *J. Appl. Meteorol.*, 35, 1362–1369, 1996.
- Chernykh, I., Alduchov, O., and Eskridge, R.: Trends in low and high cloud boundaries and errors in height determination of cloud boundaries, *Bull. Am. Meteorol. Soc.*, 82, 1941–1947, 2001.
- Chernykh, I., Alduchov, O., and Eskridge, R.: Comments on “Trends in low and high cloud boundaries and errors in height determination of cloud boundaries” – Reply, *Bull. Am. Meteorol. Soc.*, 84, 241–247, doi:10.1175/BAMS-84-2-241, 2003.
- Clothiaux, E., Ackerman, T., Mace, G., Moran, K., Marchand, R., and Miller, M.: Objective determination of cloud heights and radar reflectivities using a combination of active remote sensors at the ARM CART sites, *J. Appl. Meteorol.*, 39, 645–665, 2000.
- Crewell, S., Bloemink, H., Feijt, a., Garcia, S., Jolivet, D., Krasnov, O. A., Garcia, S. G., Van Lammeren, a., Löhnert, U., Van Meijgaard, E., Meywerk, J., Quante, M., Pfeilsticker, K., Schmidt, S., Scholl, T., Simmer, C., Schröder, M., Trautmann, T., Venema, V., Wendisch, M., and Willén, U.: The BALTEX Bridge Campaign – An integrated approach for a better understanding of clouds, *Bull. Am. Meteorol. Soc.*, 85, 1565–1584, doi:10.1175/BAMS-85-10-1565, 2004.
- de Haan, S., Bailey, L. J., and Können, J. E.: Quality assessment of Automatic Dependent Surveillance Contract (ADS-C) wind and temperature observation from commercial aircraft, *Atmos. Meas. Tech.*, 6, 199–206, doi:10.5194/amt-6-199-2013, 2013.
- Dimitrieva-Arrago, L. R. and Koloskova, L. F.: On approximate cloud boundary distribution method, *Meteorol. Hydrol.*, N6, 47–52, 1969.
- Dimitrieva-Arrago, L. R. and Shatunova, M. V.: The Approximate Method of the Cloud Boundaries Definition and its Vertical Distribution Restoration, *Research Activities in Atmospheric and Ocean Modeling*, 28, 4.5–4.6, 1999.
- Eresmaa, N., Karppinen, A., Joffe, S. M., Räsänen, J., and Talvitie, H.: Mixing height determination by ceilometer, *Atmos. Chem. Phys.*, 6, 1485–1493, doi:10.5194/acp-6-1485-2006, 2006.
- Flores, F., Rondanelli, R., Diaz, M., Querel, R., and Mundnich, K.: The life cycle of a radiosonde. *Bull. Am. Meteorol. Soc.*, 94, 187–198, 2013.
- Heintzenberg, J. and Charlson, R. J.: Clouds in the perturbed climate system: their relationship to energy balance, atmospheric dynamics, and precipitation, The MIT Press, Cambridge, Massachusetts, London, 2009.
- Illingworth, A., Hogan, R., O’Connor, E., Bouniol, D., Brooks, M., and Delanoe, J.: Cloudnet – Continuous evaluation of cloud profiles in seven operational models using ground-based observations, *Bull. Am. Meteorol. Soc.*, 88, 883–898, 2007.
- Jin, X., Hanesiak, J., and Barber, D.: Detecting cloud vertical structures from radiosondes and MODIS over Arctic first-year sea ice, *Atmos. Res.*, 83, 64–76, 2007.
- L’Ecuyer, T. and Jiang, J.: Touring the atmosphere aboard the A-Train, *Phys. Today*, 63, 36–41, 2010.
- Mather, J. and Voyles, J.: The ARM Climate Research Facility, A Review of Structure and Capabilities, *Bull. Am. Meteorol. Soc.*, 94, 377–392, 2013.
- Minnis, P., Yi, Y. H., Huang, J. P., and Ayers, K.: Relationships between radiosonde and RUC-2 meteorological conditions and cloud occurrence determined from ARM data, *J. Geophys. Res.*, 110, 1–19, 2005.
- Moninger, W. R., Mamrosh, R. D., and Pauley, P. M.: Automated meteorological reports from commercial aircraft, *Bull. Am. Meteorol. Soc.*, 84, 203–216, doi:10.1175/BAMS-84-2-203, 2003.
- Morris, V.: Vaisala Ceilometer (VCEIL) Handbook, ARM Clim. Res. Facil., 23 available at: http://www.arm.gov/publications/tech_reports/handbooks/vceil_handbook.pdf?id=25 (last access: 9 April 2014), 2012.
- Naud, C. M., Muller, J. P., and Clothiaux, E. E.: Comparison between active sensor and radiosonde cloud boundaries over the ARM Southern Great Plains site, *J. Geophys. Res.*, 108, 1–12, 2003.
- Nowak, D., Ruffieux, D., Agnew, J., and Vuilleumier, L.: Detection of fog and low cloud boundaries with ground-based remote sensing systems, *J. Atmos. Ocean. Technol.*, 25, 1357–1368, 2008.
- Poore, K., Wang, J., and Rossow, W.: Cloud Layer Thicknesses from a Combination of Surface and Upper-Air Observations, *J. Climate*, 8, 550–568, 1995.

- Qian, Y., Long, C. N., Wang, H., Comstock, J. M., McFarlane, S. A., and Xie, S.: Evaluation of cloud fraction and its radiative effect simulated by IPCC AR4 global models against ARM surface observations, *Atmos. Chem. Phys.*, 12, 1785–1810, doi:10.5194/acp-12-1785-2012, 2012.
- Schwartz, B. and Benjamin, S. G.: A comparison of temperature and wind measurements from ACARS-Equipped Aircraft and Rawinsondes, *Weather Forecast.*, 10, 528–544, doi:10.1175/1520-0434(1995)010<0528:ACOTAW>2.0.CO;2, 1995.
- Seidel, D. and Durre, I.: Comments on “Trends in low and high cloud boundaries and errors in height determination of cloud boundaries”, *Bull. Am. Meteorol. Soc.*, 84, 237–240, doi:10.1175/BAMS-84-2-237, 2003.
- Sun, B., Reale, A., Schroeder, S., Seidel, D. J., and Ballish, B.: Toward improved corrections for radiation-induced biases in radiosonde temperature observations, *J. Geophys. Res.-Atmos.*, 118, 4231–4243, 2013.
- Wang, J. and Rossow, W.: Determination of Cloud Vertical Structure from Upper-Air Observations, *J. Appl. Meteorol.*, 34, 2243–2258, 1995.
- Wang, J. and Rossow, W.: Effects of cloud vertical structure on atmospheric circulation in the GISS GCM, *J. Climate*, 11, 3010–3029, 1998.
- Wang, J., Rossow, W., Uttal, T., and Rozendaal, M.: Variability of cloud vertical structure during ASTEX observed from a combination of rawinsonde, radar, ceilometer, and satellite, *Mon. Weather Rev.*, 127, 2484–2502, 1999.
- Wang, J., Rossow, W., and Zhang, Y.: Cloud vertical structure and its variations from a 20-yr global rawinsonde dataset, *J. Climate*, 13, 3041–3056, 2000.
- Wang, J. H., Carlson, D. J., Parsons, D. B., Hock, T. F., and Lauritsen, D.: Performance of operational radiosonde humidity sensors in direct comparison with a chilled mirror dew-point hygrometer and its climate implication, *Geophys. Res. Lett.*, 30, 11-1–11-4, 2003.
- World Meteorological Organization (WMO): International Cloud Atlas, Manual on the observation of clouds and other meteors, WMO, I, 1975.
- Xi, B., Dong, X., Minnis, P., and Khaiyer, M.: A 10 year climatology of cloud fraction and vertical distribution derived from both surface and GOES observations over the DOE ARM SPG site, *J. Geophys. Res.*, 115, 1–12, doi:10.1029/2009JD012800, 2010.
- Yi, Y. H., Minnis, P., Ayers, J. K., Huang, J. P., Doelling, D. R., Khaiyer, M. M., and Nordeen, M. L.: Relationships Between Meteorological Conditions and Cloud Properties Determined from ARM Data, 14th ARM Science Team Meeting Proceedings, Albuquerque, New Mexico, 1–18, 2004.
- Zhang, J., Chen, H., Li, Z., Fan, X., and Peng, L.: Analysis of cloud layer structure in Shouxian, China using RS92 radiosonde aided by 95 GHz cloud radar, *J. Geophys. Res.*, 115, 1–13, 2010.
- Zhang, J., Chen, H., Bian, J., Xuan, Y., and Duan, Y.: Development of Cloud Detection Methods Using CFH, GTS1, and RS80 Radiosondes, *Adv. Atmos. Sci.*, 29, 236–248, doi:10.1007/s00376-011-0215-4, 2012.
- Zhang, J., Li, Z., Chen, H., and Cribb, M.: Validation of a radiosonde-based cloud layer detection method against a ground-based remote sensing method at multiple ARM sites, *J. Geophys. Res.*, 118, 846–858, doi:10.1029/2012JD018515, 2013.